National Conference with International Participation
ENGINEERING MECHANICS 2007
Svratka, Czech Republic, May 14 – 17, 2007

OPTIMIZATION OF THE COMMUTER AIRCRAFT WING STIFFNESS CHARACTERISTICS CONSIDERING REQUIREMENT OF AEROELASTIC STABILITY AT THE CERTIFICATION SPEED

J.Čečrdle *

Summary: *The submitted paper deals with aeroelastic optimization. It gives a summary of theory with special regard to the aeroelasticity. Main part describes optimization of the aircraft wing stiffness characteristics to ensure the flutter stability below the certification speed. The problem is represented by the wing tip tank filling, which causes significant change of the modal characteristics and so the flutter stability characteristics. The task aim is to ensure flutter stability below the certification speed for whole range of the tip tank filling.*

1. Introduction

The presented task is demonstrated on the structure of the Czech small twin turboprop commuter aircraft for 19 passengers. One of the last modifications from the eighties of the last century was based on the installation of wing tip tanks (fig.1). Tip tanks obviously influence the wing aerodynamics; also structural strength aspects are remarkable. The most important aspect, which is not primarily visible is influence of the tip tanks to aeroelastic especially flutter stability characteristics. Wing tip tanks represent significant mass placed at the aeroelastically sensitive position. The fuel drawing from the tip tanks strongly impacts the mass characteristics and so the modal characteristics of the whole wing. Also the possible influence to the non-stationary aerodynamic forces should be mentioned. During development of the aircraft modification with tip tanks, the large analytical studies and experiments on the dynamically similar (aeroelastic) model were performed. Most of experiments were performed on the aeroelastic model of the isolated wing (fig.2). Both analyses and experiments proved the significant influence of the tip tanks filling to the bending – torsion flutter characteristics. The critical combination of two modes (2^{nd} wing bending, 1^{st} wing torsion) was found. While the flutter speed for the full and empty tank configurations were high enough, for the partial filling the flutter speed decreased (from both sides) and reached the area of requested aeroelastic stability (below the certification speed). The critical level of the tip tanks filling was 60%. For that reason, initially designed tip tank had to be redesigned; especially the tip tank volume was decreased.

Fig.1 – Czech small commuter aircraft

* Ing. Jiří Čečrdle, Ph.D.: Aeronautical Research and Test Institute (VZLU); Beranových 130; 199 05 Praha – Letňany; tel.:(+420) 225 115 123; fax:(+420) 283 920 018; e-mail: cecrdle@vzlu.cz

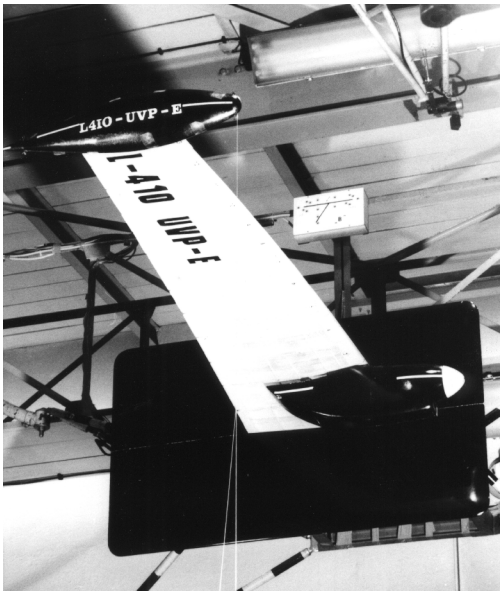

Fig.2 – Aeroelastic model of the wing – engine component

Considering the above described flutter behaviour, this structure was chosen for research and development of methods and procedures for optimization of the structural characteristics regarding the flutter behaviour. Analyses were performed using structural data (inertia and stiffness characteristics, geometry) of the aeroelastic model. The main aim of the presented task is to make an optimization of the stiffness characteristics in order to increase the flutter speed out of the required stability area, it means above the certification speed for whole range of the tip tank filling.

It should be reminded, that the aeroelastic model was scaled down from the full-scale aircraft, the length scale was 0.2 ; the velocity scale 0.18 . The aircraft certification speed scaled down to the aeroelastic model was 31.7 $m.s^{-1}$.

2. Theoretical Background

Optimization is a process of the structure changes aimed to make an improvement considering determined conditions and parameters. Basically optimization is a mathematical algorithm of seeking the optimal parameters combination to minimize the objective function respecting determined limitations and conditions. Following text describes main terms used in optimization.

Design Variable is a quantity, which is changeable. It is possible to specify both boundary values and change rate for an optimization cycle. It is not required to correspond to the FE model property; it may become a combination of several properties. Design variables can be dependent one another.

Design Property is a FE model property relating to the design variable. In the case of shape optimization may become a grid position. Also boundary values may be specified. It may become either a linear combination of design variables ($p_j = C_0 + \sum_i C_i x_i$) or a general, also non-linear function ($p_j = f(\{x\},\{C\})$), and also a set of discrete values is allowed.

Design Response may become either objective function or design constraint. It may be either linear or non-linear combination of design variables, other design responses, sets of discrete values and constants etc. Character of design responses determines the optimization algorithm (linear, non-linear). **Objective function** is a scalar quantity, which is minimized during optimization (maximization is mathematically realized as minimization of reciprocal value). **Design Constraint** is a quantity or function defined as condition, which must be held. It may be an inequality (for example $h_i(\vec{x}) \le 0$), equality (for example $h_i(\vec{x}) = 0$), side constraints (for example $x_i^I \le x_i \le x_i^U$) etc.

Optimization procedures belong to the family of methods called “gradient-based”, since it determine the gradients of the objective function and constraints to determine a direction of searching for the optimum in the design space. Then it proceeds in that direction as far as they can go. After that it investigates if we are at the optimum point, if not the process is repeated until can make no more improvement of the objective without violating some constrain.

In connection with the optimization should be noted a sensitivity analysis. The sensitivity coefficients are defined as the rate of change of a particular design response with respect to a change in a design variable:

$$(\mathrm{DSCM2})_{ij} = \left(\frac{\partial r_j}{\partial x_i} \right)_{x \to 0} \tag{1}$$

Sensitivity analysis is useful to specify suitable design variables; it means those ones, which have big sensitivities to the objective function.

Optimization may cover various types of analyses. In this paper, we will not deal with the statics, normal or complex modes, buckling, frequency or transient responses, we will concentrate on the aeroelasticity.

For the static aeroelasticity, apart from the ordinary design responses like displacement, strain, stress, force, etc. the two specific types are applicable (trim variables and stability derivatives). For the dynamic aeroelasticity (flutter) solution are the design responses represented by the damping values for a specific mode, density, Mach number and velocity. Obviously synthetic responses defined as a function of other design responses, design variables, constants etc. are allowed. Trim variables responses can be used for applications like “required control surface deflection for a specific maneuver”, “required angle of attack for specific flight regime” etc. Stability derivatives responses can be used for applications like “maximal lift curve slope” etc., also synthetic design responses like roll rate can be specified as division of two stability derivatives:

$$\frac{\omega_x b}{2V\delta_a} = -\frac{c_L^{\delta_a}}{c_L^{\omega_x}} \tag{2}$$

A solution of static aeroelastic divergence is also allowed.

For the flutter solution, the design response is represented by the total damping of the structure for a selected mode, air density (ρ), Mach number and velocity (V). Obviously synthetic responses like “maximal damping value in the velocity range” for elimination of “hump mode instability” and many other applications can be prepared. It is obvious, that usage of such advanced synthetic applications assumes a knowledge regarding the flutter behavior of the structure.

For the optimization purposes, only the PK method and derived PKNL and PKS methods are applicable. The basic flutter equation in modal coordinates is:

$$\left[M_{hh} p^2 + \left(B_{hh} - \frac{1}{4} \frac{\rho c V Q_{hh}^{Im}}{k} \right) p + \left(K_{hh} - \frac{1}{2} \rho V^2 Q_{hh}^{Re} \right) \right] \{u_h\} = 0 \tag{3}$$

M_{hh}, B_{hh} and K_{hh} are modal mass, damping and stiffness matrices respectively. Aerodynamic loads are incorporated into damping and stiffness matrices. Aerodynamic matrices are dependent on the reduced frequency (k) at a gentle rate. All matrices are real, Q_{hh}^{Re} and Q_{hh}^{Im}

are real and imaginary part of complex aerodynamic matrix Q_{hh}. The decay rate coefficient is defined in connection with the complex eigenvalue:

$$p = \omega(\gamma \pm j) = p^{Re} + jp^{Im} \tag{4}$$

Flutter sensitivities are computed as rate of change of the transient decay coefficient γ with respect to changes in design variables $(\partial\gamma/\partial x_i)$.

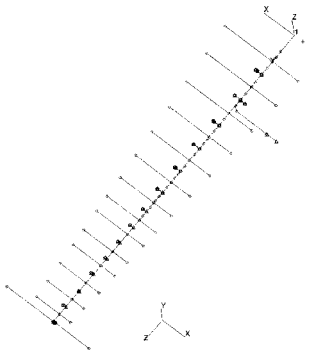

Fig.3 – Structural FE model

3. FE Model

The FE model was prepared according the hardware model structural data (Fiala, Maleček, 1985). It corresponds to the described hardware model structure. (elements BAR, CONM2, CELAS, conditions RBE2, MPC). Model is fixed at the wing root. Since the main aeroelastic problem is bending – torsion flutter, the aileron is not modeled separately. According to the hardware model, engine is considered as a concentrated mass with the vertical bending stiffness only. Fuel in the wing tank is considered at the level of 75,1 %. Fuel in the wing tip tank is modeled for the several filling levels. It represents the main parameter of analyses. The structural model is shown in the fig.3. The aerodynamic model is prepared for the Wing – Body Interference Aerodynamic Theory. The wing and spliter (to prevent the induced effects at the wing root) are modeled as Doublett – Lattice macroelements (CAERO1), the nacelle and tip tank are modeled as the Slender and Interference Bodies (CAERO2). Structural and aerodynamic parts are connected by means of the beam splines, spliter is grounded via surface spline. The aerodynamic part of the model is shown in fig.4. Model was verified using results of the modal tests (Černý, Hlavatý, Zamrazil, 1985) and wind tunnel flutter tests (Maleček, 1987). Experimental modal characteristics and flutter characteristics were compared with corresponding analytical results (Čečrdle, 2002). The analysis and experimental results agreement have been found on the acceptable level.

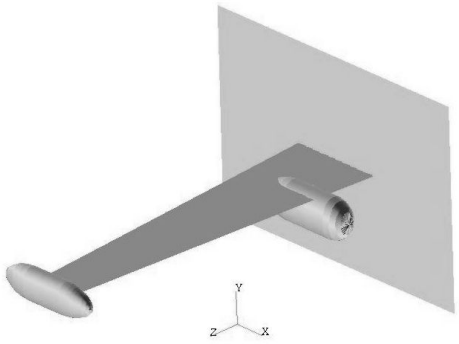

Fig.4 – Aerodynamic FE model

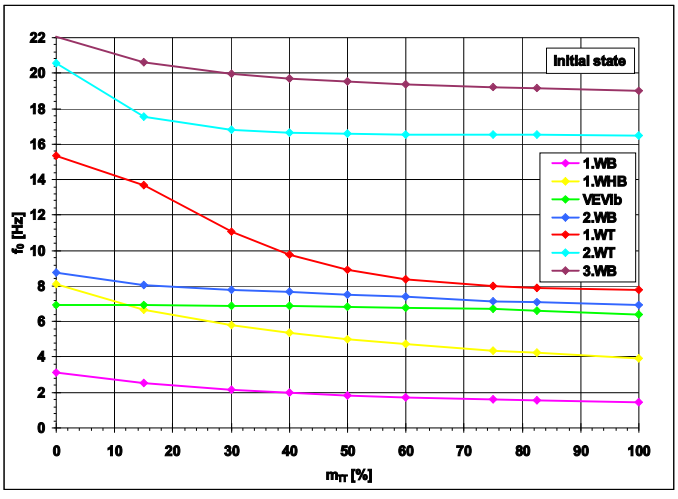

Fig.5 – Natural frequencies – initial state

4. Initial state

The aim of the initial state calculations was to define aeroelastic

Tab.1 – Flutter speeds and frequencies – initial state

m_{TT} [%]	BWE		BTW	
	V_{FL} [m.s^{-1}]	f_{FL} [Hz]	V_{FL} [m.s^{-1}]	f_{FL} [Hz]
0	57.9	6.5	55.1	10.7
15	68.2	6.2	50.0	9.8
30	71.3	5.7	39.8	9.3
40	69.3	5.3	32.0	8.7
50	71.2	5.0	25.6	8.3
60	71.9	4.7	22.3	8.0
75	75.7	4.3	32.1	7.6
82.5	78.2	4.1	-	-
100	-	-	-	-

instabilities to have a comparative set of the data to compare with the optimized structure. It is also used to define the optimization strategy. Calculations were performed for a several tip tank filling levels m_{TT} = (0; 15; 30; 40; 50; 60; 75; 82.5; 100) %. Modal analysis was performed by means of the Lanczos method for 7 mode shapes (1st wing bending – 1.WB; 1st wing horizontal bending – 1.WHB; engine vertical vibrations – EVVib; 2nd wing bending – 2.WB; 1st wing torsion – 1.WT; 2nd wing torsion – 2.WT; 3rd wing bending – 3.WB; results are presented in the fig.5. There is a visible approaching trend of the 2.WB and 1.WT modes frequencies for the specific range of the tip tank filling in the figure. This fact, as described later, causes a flutter speed decreasing. The flutter analyses were performed for a set of mentioned 7 modes by means of the PK (British) method for velocities up to 80 m.s^{-1}. Mach number was considered Ma = 0, air density ρ = 1.225 kg.m^{-3}. Structural damping was considered by viscous model, damping ratio of 0,002 was set for whole frequency range considering the values given from ground vibration tests for specific modes. The two types of flutter instability occurred:

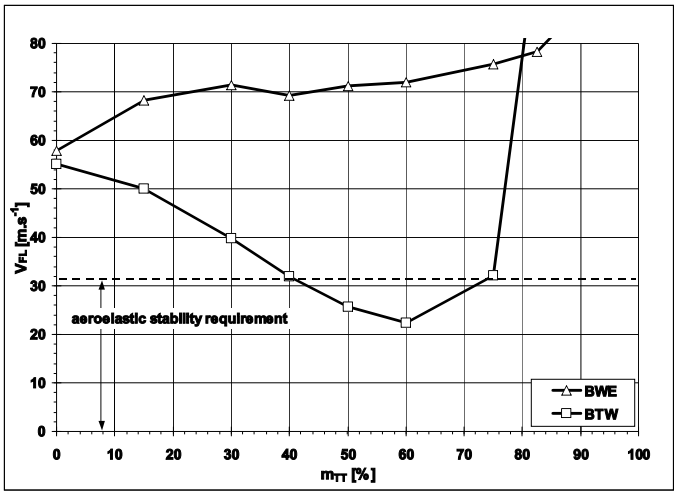

Fig.6 – Flutter speeds – initial state

1) Bending – (torsion) – wing - engine fluter (BWE)

The critical mode shape combination is 1.WB + EVVib, also 1.WT have a noticeably destabilizing influence. The engine is vibrating in opposite phase with the wing. The flutter speed is sufficiently above the certification speed for a whole range of the tip tank filling.

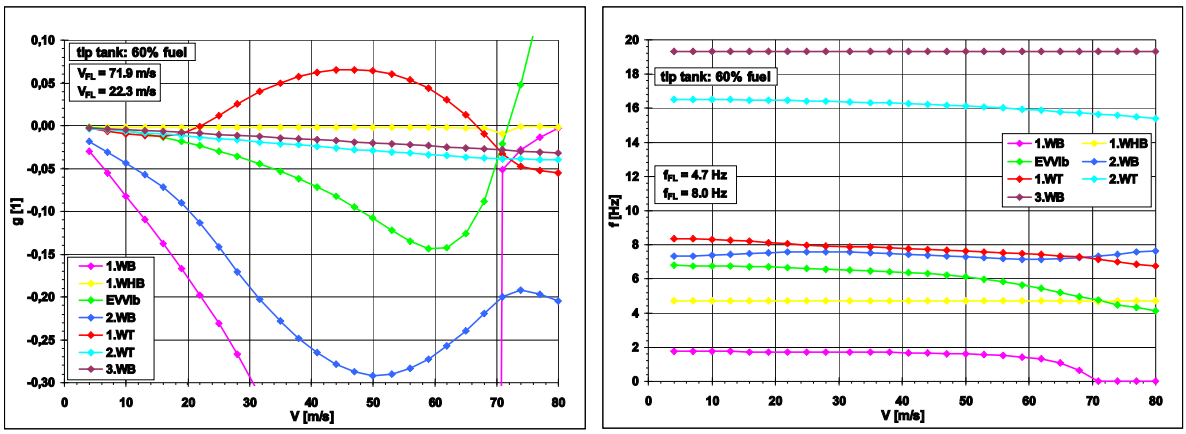

Fig.7ab – V-g-f diagram – initial state – critical tip tank filling

2) Bending – torsion – wing fluter (BTW)

The critical mode shape combination is 2.WB + 1.WT. Engine is vibrating together with the wing. The flutter speed reaches an area of required aeroelastic stability (below the certification speed) for specific range of the tip tank filling. This is a crucial aeroelastic problem of the structure. The optimization should lead to improve flutter stability in this field.

List of the flutter speed and flutter frequencies is given in the tab.1 and in the fig.6. As visible from the fig.6, the critical level of the tip tank filling is m_{TT} = 60%. The V-g-f diagram is presented in the fig.7, the critical root (1.WT) has a character of instable hump mode.

5. Optimization task definition

The optimization aim was to improve the structure aeroelastic stability, to increase the flutter speed above the certification speed of 31.7 $m.s^{-1}$ by means of changing the stiffness characteristics. Changes should be as minimal as possible.

The design objective represents the condition of V_{FL} = 31.7 $m.s^{-1}$ for the critical root (1.WT). It is realized by means of squared damping value for mode #5 and velocity of 31.7 $m.s^{-1}$ minimization. Design constrains must satisfy demands of no other instability below the velocity of 31.7 $m.s^{-1}$. Regarding the numerical complications with setting the zero damping value, the condition was defined as ((g-0,03)/0,1)<-0,3 for remaining modes (#1,2,3,4,6,7) and velocity of 31.7 $m.s^{-1}$.

Design variables were specified at two levels. The first one is a global parameters level, it means that the parameters change is the same for the whole structure; in fact it is a scale factor. In this case, two design variables were set, for clarity both values were 100. Design variables were connected to the E and G modulus; relations were linear with constants of E/100 and G/100 respectively.

The second, more general possibility of design variables specification is a local parameters level; it means that in general, the changes may be different for any specific element. For each element, three design variables representing vertical bending stiffness (EI_y), horizontal bending stiffness (EI_z) and torsional stiffness (GI_k) were specified. Design variables were connected to the cross-section characteristics of each element (I1, I2, J), relations were linear with constants of 1/E and 1/G respectively.

In both cases, the maximal allowed parameter change during one optimization cycle was set

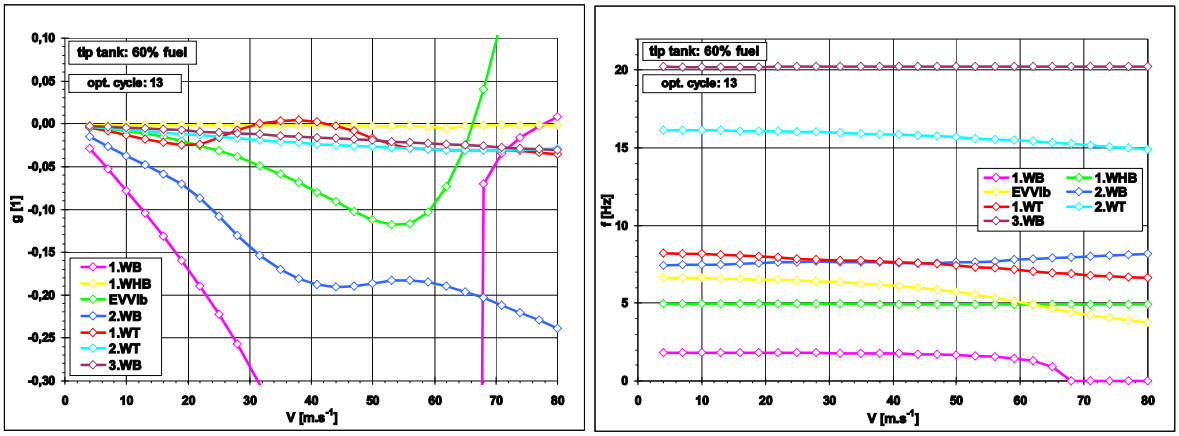

Fig.8ab – V-g-f diagram – optimized – global parameters – critical tip tank filling

to ±1%. Firstly the optimization was performed for the critical tip tank filling level (60%). As described in the chapter 6 and 7, the optimization was successful for both design variable levels. After that, the optimized structure was applied to other tip tank filling levels. Unfortunately, the unacceptable instability occurred for the filling level of 50%. The next testing optimization calculations indicated, that the stiffness changes for m_{TT}=60% and m_{TT}=50% were the opposite orientation (decreasing / increasing) as for m_{TT}=60%. For that reason, some kind of composite step-by-step optimization procedure was necessary to ensure the required level of stability for a whole range of the tip tank filling. The results of mentioned optimization are described in the chapter 8.

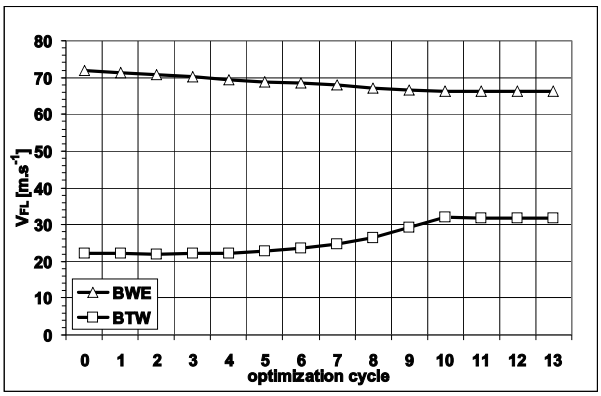

Fig.9 – Flutter speed – optimization process

6. Optimization for critical tip tank filling – global parameters

The optimization was performed in 13 optimization cycles. The bending stiffness was increased (scale factor 1.0964), torsional stiffness was decreased (scale factor 0.9048). Bending modes frequencies increased, torsional modes frequencies decreased, engine vibration frequency slightly changed due to the wing torsion. The V-g-f diagram of the optimized structure is presented in the fig.8. The flutter speed process is presented in the fig.9. Firstly the height of the 1.WT hump was reduced, then the BTW instability flutter speed get increase above the 31.7 m.s^{-1}, the last stage is a final tuning to the appropriate value. BWE instability flutter speed slightly decreased, considering the large reserve, such decreasing is acceptable.

7. Optimization for critical tip tank filling – local parameters

The optimization was performed in 12 optimization cycles. The vertical bending and torsional stiffness changes are documented in the fig.10ab. The vertical bending stiffness parameters increased along a whole span by about 8%, horizontal bending stiffness parameters increased mainly in the tip part maximally by 5%, torsional stiffness parameters increased in the root part by about 8.5%, otherwise it decreased by about 8.5%. Changes of the modal characteristics correspond to the global parameters optimization. Changes are slightly lower

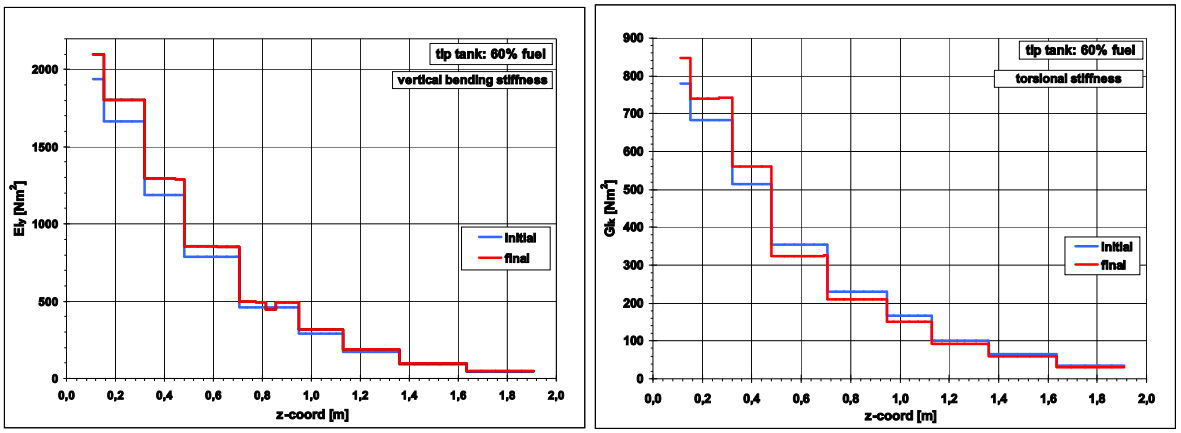

Fig.10ab – Parameters changes – local parameters – critical tip tank filling

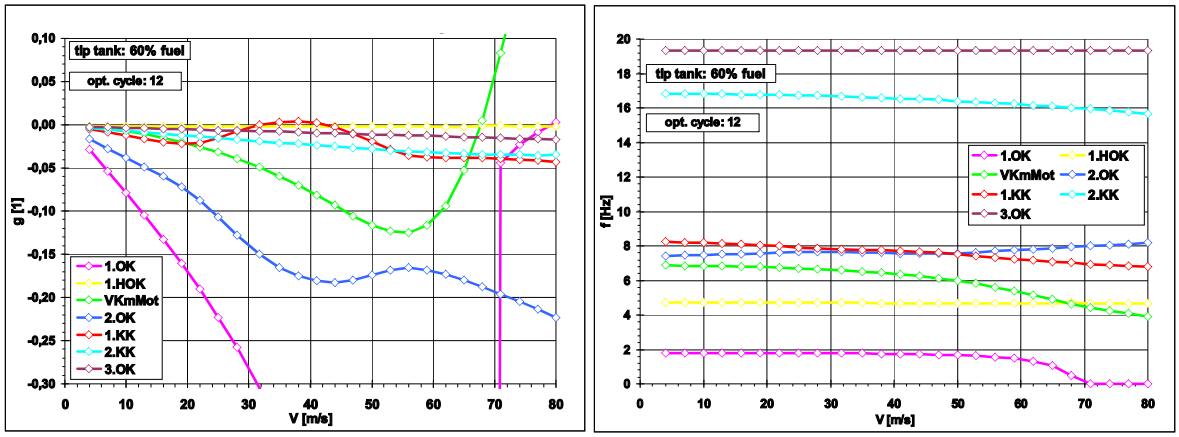

Fig.11ab – V-g-f diagram – optimized – local parameters – critical tip tank filling

than at the previous example. The V-g-f diagram of the optimized structure is presented in the fig.11. The flutter speed process is presented in the fig.12; it corresponds to the global parameters case.

8. Optimization for whole range of the tip tank filling

The optimization was performed in 5 steps. Design variables were specified at the local level. In the separate step, just one type of stiffness was used (vertical bending or torsional). The optimization was performed for every tip tank filling levels, except those ones, which have enough stability reserve. The final state of each step was determined as a compromise solution.

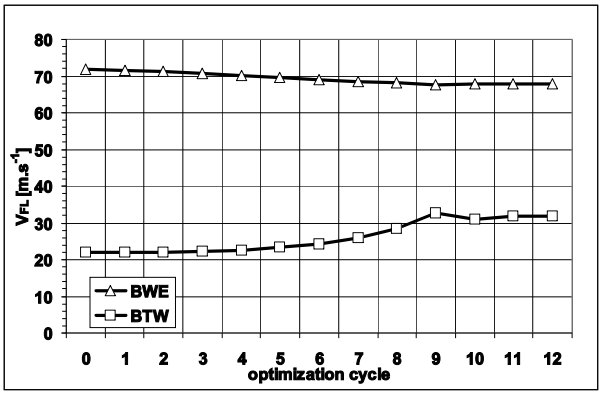

Fig.12 – Flutter speed – optimization process

In the first step, the torsional stiffness parameters were used as design variables, the objective function and design constraint were defined as described in the chapter 5. A similar approach was used also at the second step, just the objective function was specified as minimization of the squared value of the maximal damping at the selected velocity range. In the next two steps, the vertical

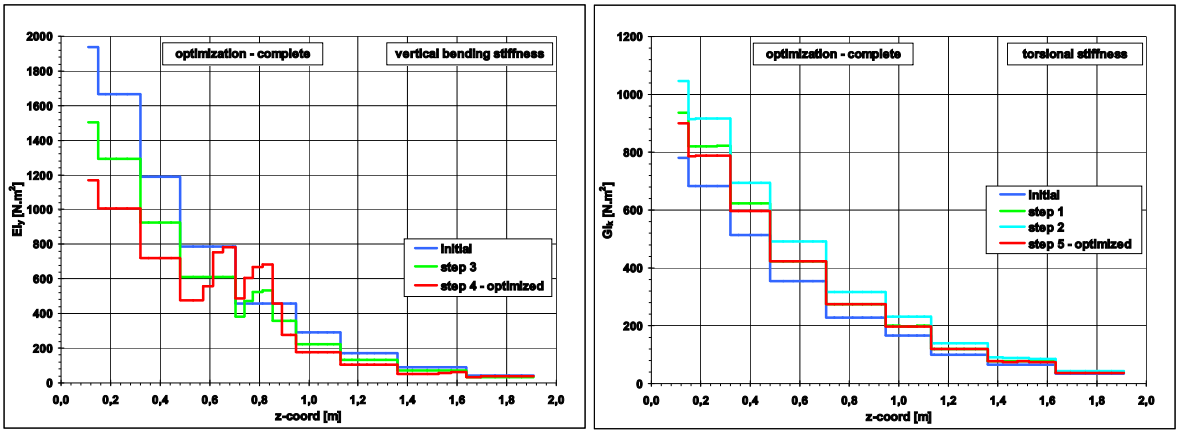

Fig.13ab – Parameters changes – whole tip tank filling range optimization

stiffness parameters were used as design variables and the initial type of the objective function were used. After that, the required level of aeroleastic stability has been reached. The last step was used to approach the flutter speed of the most critical tip tank filling to the value of 31.7 $m.s^{-1}$. The torsional stiffness was used as a global design variable.

Stiffness parameters changes process during the optimization procedure is demonstrated in the fig.13ab. Parameters changes are relatively high; especially bending stiffness changes would be difficult to realize on the full-scale structure. In spite of that the primary objective, it means to ensure required level of flutter stability was reached. Changes of natural frequencies are demonstrated in the fig.14.

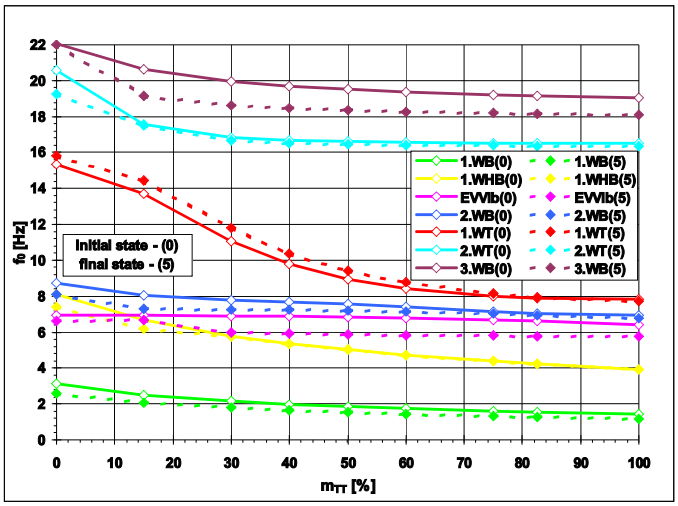

Fig.14 – Natural frequencies – comparison initial / final state

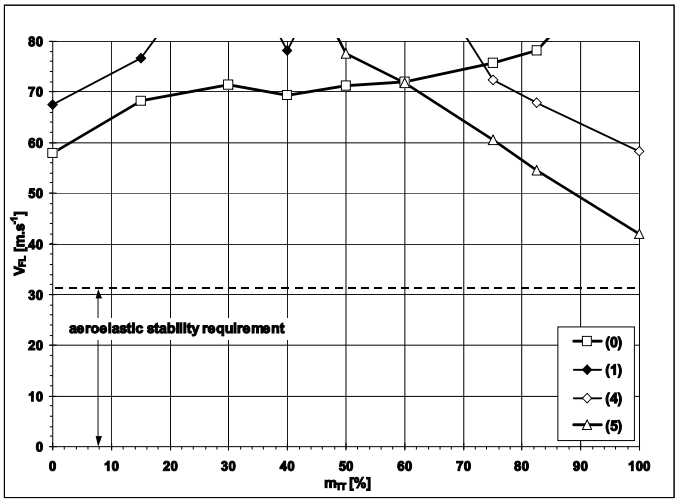

Fig.15 – Flutter speeds - BWE instability – comparison initial (0) / final (5) state

Tab.2 – BWE flutters speeds and frequencies – optimized structure

m_{TT} [%]	V_{FL} [$m.s^{-1}$]	f_{FL} [Hz]
0	---	---
15	---	---
30	---	---
40	---	---
50	77,6	6,2
60	71,8	6,2
75	60,6	6,2
82,5	54,6	6,2
100	42,0	6,2

As mentioned in the chapter 5, there were two flutter instabilities found. BWE instability on the optimized structure becomes a different character. The critical combination of modes includes 2.WB, EVVib and 1.WT. The 1.WB mode was replaced by 2.WB due to decreasing of the vertical bending stiffness and changes around the engine. BWE instability flutter speeds are sufficiently above the certification speed of 31.7 $m.s^{-1}$ as demonstrated in the fig.15. BWE instability flutter speeds and frequencies for the optimized structure are also summarized in the tab.2.

Critical instability type was the BTW flutter. This flutter type on the optimized structure have not changed the character, flutter speeds are above the certification speed, in the most critical level of the tip tank filling (m_{TT} =75%) flutter speed is reaching the value of 31.7 $m.s^{-1}$. Flutter speeds and frequencies at all steps of the optimization process are summarized in the tab.3 and graphically in the fig.16. The V-g-f diagram for the optimized structure, tip tank filling of 60% is presented in the fig.17.

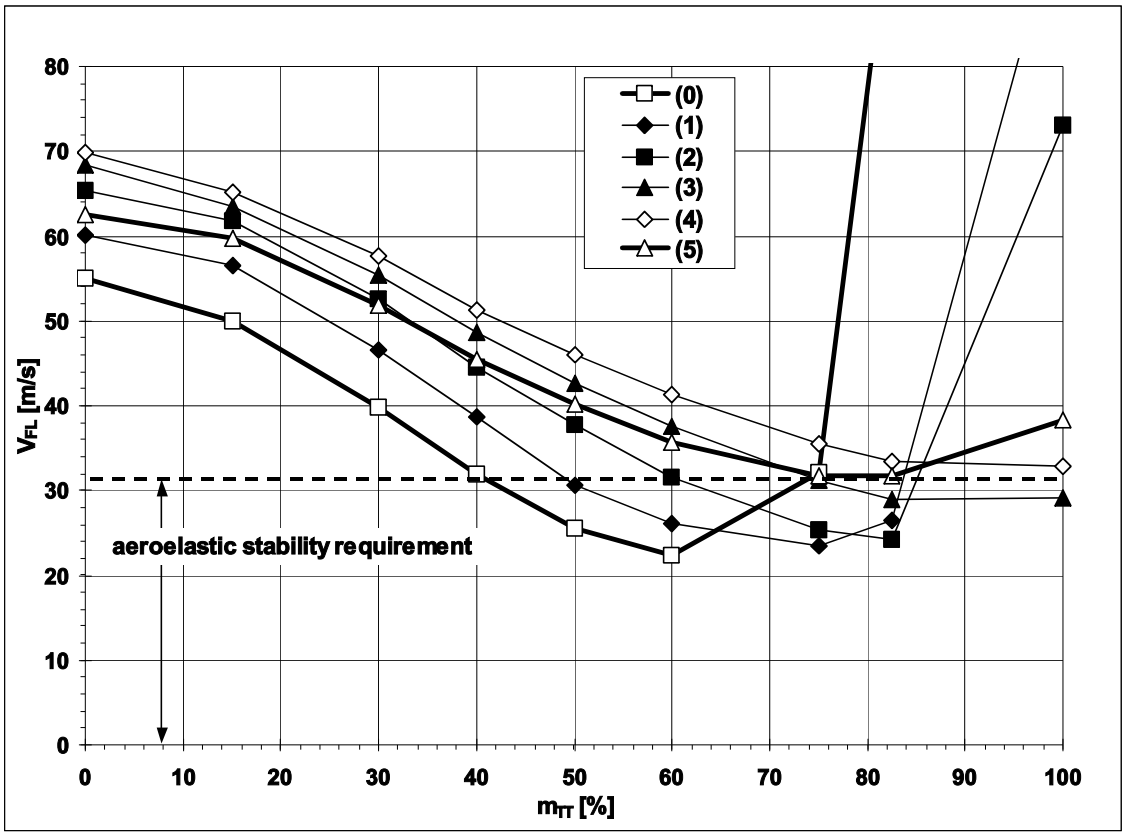

Fig.16 – BTW instability – flutter speeds over the optimization process

Tab.3 – BWE instability – flutter speeds and frequencies over optimization steps

	Optimization step											
	(0)		(1)		(2)		(3)		(4)		**(5)**	
m_{TT} [%]	V_{FL} [$m.s^{-1}$]	f_{FL} [Hz]	V_{FL} [$m.s^{-1}$]	f_{FL} [Hz]	V_{FL} [$m.s^{-1}$]	f_{FL} [Hz]	V_{FL} [$m.s^{-1}$]	f_{FL} [Hz]	V_{FL} [$m.s^{-1}$]	f_{FL} [Hz]	V_{FL} [$m.s^{-1}$]	f_{FL} [Hz]
0	**55,1**	**10,7**	60,1	11,2	65,3	12,3	68,3	12,2	69,8	12,1	**62,6**	**10,9**
15	**50,0**	**9,8**	56,5	10,3	61,7	10,8	63,4	10,5	65,2	10,2	**59,8**	**9,6**
30	**39,8**	**9,3**	46,6	9,6	52,6	9,9	55,4	9,6	57,7	9,5	**51,8**	**9,0**
40	**32,0**	**8,7**	38,6	9,1	44,6	9,5	48,6	9,1	51,3	8,9	**45,4**	**8,5**
50	**25,6**	**8,3**	30,7	8,7	37,7	9,0	42,7	8,7	46,0	8,6	**40,1**	**8,2**
60	**22,3**	**8,0**	26,1	8,4	31,6	8,7	37,5	8,5	41,3	8,3	**35,7**	**8,0**
75	**32,1**	**7,6**	23,5	8,0	25,3	8,3	31,1	8,2	35,4	8,0	**31,7**	**7,7**
82,5	**---**	**---**	26,4	7,8	24,2	8,2	29,0	8,0	33,5	7,9	**31,8**	**7,6**
100	**---**	**---**	---	---	73,1	12,4	29,2	7,8	32,9	7,7	**38,4**	**7,4**

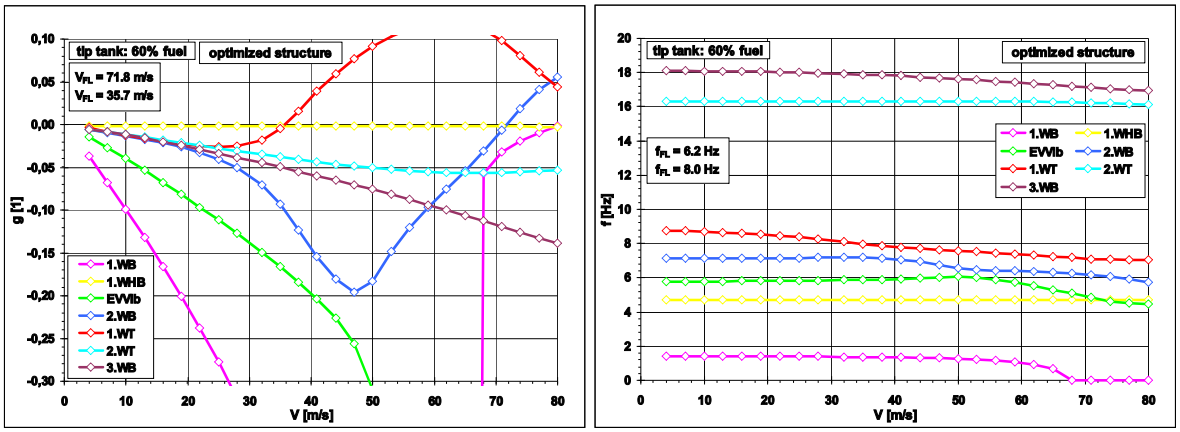

Fig.17ab – V-g-f diagram – optimized – tip tank filling 60%

9. Conclusion

The submitted paper deals with the optimization of the commuter aircraft wing – engine component stiffness characteristics regarding the requirements of the flutter stability. First part describes the theoretical aspects; fundamental terms and principles are outlined. Special attention is paid to the optimization in the aeroelasticity. Second, practical part documents the structure optimization. The optimization task is defined to ensure flutter stability on the required level, it means above the certification speed. In the first phase, the task is solved for a selected mass configuration defined by the tip tank filling level, which is critical from the flutter stability point of view. The main emphasis is focused to the enlarged task with demand to ensure the required level of stability for a whole range of the tip tank filling. The required stability level should be reached by means of the minimal possible changes of the stiffness characteristics.

The FE model, used methods, modal and flutter characteristics of the initial structure are documented. The optimization for the selected tip tank filling level of 60% fuel was performed by means of both global and local parameters level. The solution was successful for both approaches, changes of the vertical bending and torsional stiffness were around 9 – 10% for global parameters and maximally around 8,5% for local parameters respectively. The optimized structure was applied to remaining tip tank filling levels; unfortunately it didn't meet the requirements for the other tip tank filling level of 50%. The followed-up testing calculations proved, that mentioned mass configurations would demand the opposite changes of stiffness parameters.

From that reasons, the optimization for a whole range of the tip tank filling was performed at the several steps, the selected parameters were either vertical bending or torsional stiffness, both ones on the local level. The resultant parameters changes were combined from calculations for a several tip tank filing levels. Finally, the required level of the flutter stability has been reached for all the mass configurations. It must be said, that the parameters changes were much higher, than for the previous task, it means up to 20% for a torsional stiffness and around 40% for a vertical bending stiffness.

It should be noted, that such a changes would be difficultly feasible to the full-scale aircraft, also any change of the stiffness must influence the mass characteristics. At the development phase of the aircraft, the flutter stability problems were solved out by considerable decreasing of the tip tank volume and by further design changes.

It is obvious, that the optimization task applied for example to configurations up to filing of 70% would represent much easier task and required parameters changes would be much lower. In connection with that, the structural damping regarding issues should be noted. The structural damping ratio was set to 0,002. It corresponds to the values given from the vibration tests. Nevertheless, in general, damping ratios of the aeroelastic models are quite low; the full-scale aircraft structural damping ratios are much higher (0,02 – 0,06). It would certainly help to the better solution. In general, presented work contributed to the verification of aeroelastic optimization procedures and indicated the further research areas.

10. Acknowledgements

The paper was prepared in the frame of the project "Research on Strength of Low-weight Structures with Special Regard to Airplane Structures" funded from the Czech Ministry of Education, project number MSM 0001066903.

11. References

Heinze, P. – Schierenbeck, D. – Niemann, L. (1989) Structural optimization in View of Aeroelastic Constraints Based on MSC/NASTRAN FE-Calculation, 16th MSC European Users' Conference, paper no.15, September 1989.

Lewis, A.P. (1991) A NASTRAN DMAP Procedure for Aeroelastic Design Sensitivity Analysis, 18th MSC European Users' Conference, paper no.15, June 1991.

Moore, G.J. (1994) MSC/NASTRAN Design Sensitivity and Optimization, The Macneal-Schwendler Corporation, 1994

Čečrdle, J. (2002) Ověření modálních a flatrových charakteristik dynamicky podobného modelu křídla letounu L-410UVP-E výpočtem MKP pomocí programu MSC.NASTRAN, Setkání uživatelů – info dny MSC.Software s.r.o. 2002 – sborník, příspěvek č. 18, Brno 29.-30.5.2002, ISBN 80-238-8753-X

Fiala, J. – Maleček, J. (1985) Technická dokumentace dynamicky podobného modelu isolovaného křídla s koncovou nádrží letounu L-410 UVP-E, zpráva VZLÚ R-2247/85, 30.9.1985

Černý, O. – Hlavatý, V. – Zamrazil, M. (1985) Rezonanční zkouška dynamicky podobného modelu křídla letounu L 410 UVP-E, zpráva VZLÚ Z-2949/85, 29.3.1985

Maleček, J. (1987) Ověření dynamické stability křídla s koncovou nádrží letounu L-410 UVP-E na dynamicky podobném modelu, zpráva VZLÚ V-1586/87, 31.1.1987

Čečrdle, J. (2007) Optimalizace tuhostních charakteristik křídla dynamicky podobného modelu letounu L410UVP-E s ohledem na požadavek aeroelastické stability konstrukce při průkazné rychlosti, zpráva VZLÚ R-3954, duben 2007